This is a preprint version of the full-length proceedings paper available here:
https://doi.org/10.1117/12.2578904. Please see the publisher's website for the final version along with a video presentation

Waveguiding and dispersion properties of interband cascade laser frequency combs

L. A Sterczewski[a], M. Bagheri[1a], C. Frez[a], C. L. Canedy[b], I. Vurgaftman[b], M. Kim[c], C. S. Kim[b], C. D. Merritt[b], W. W. Bewley[b], J. Faist[d], G. Wysocki[e], and J. R. Meyer[b]

[a]Jet Propulsion Laboratory, California Institute of Technology, Pasadena, CA 91109, USA; [b]Naval Research Laboratory, Washington, DC 20375, USA; [c]Jacobs, Hanover, MD 21076, USA; [d]Institute for Quantum Electronics, ETH Zurich, 8093 Zurich, Switzerland; [e]Department of Electrical Engineering, Princeton University, Princeton, New Jersey 08544, USA;

ABSTRACT:

Mid-infrared semiconductor lasers have emerged as indispensable compact coherent sources for military and commercial applications. While much of the historical emphasis has been on maximizing the output power and/or spectral purity, a recent new focus has been on engineering these lasers to operate as optical frequency combs (OFCs) for broadband real-time spectroscopy. In particular, the combination of low-drive-power and broad gain bandwidth has made interband cascade laser (ICL) OFCs an attractive complement to quantum cascade laser OFCs operating at longer wavelengths. Moreover, ICL combs can potentially be incorporated into fully-integrated dual-comb spectrometers that employ fast, room-temperature IC photodetectors processed on the same chip.

However, the high refractive index of the ICL's GaSb substrate poses some challenges to the optical waveguiding. Because the modal index is considerably lower than that of the substrate, the optical field can penetrate the bottom cladding layer and leak into the GaSb, inducing wavelength-dependent interference that modifies the gain and group velocity dispersion (GVD) profiles. Even when the effect on lasing threshold is small, the comb properties can be adversely affected.

Using the sub-threshold Fourier transform technique, we studied ICL combs with various ridge widths, substrate thicknesses, and center wavelengths. This allowed us to evaluate the effects of modal leakage on the GVD. We find that the resonant nature of the substrate modes induces oscillations, which affect both the spectral bandwidth and the phase-locking properties above threshold. Strategies to mitigate the GVD's undesired and unpredictable spectral variation will be presented.

Keywords: interband cascade, semiconductor laser, optical mode

1. INTRODUCTION

Group velocity dispersion (GVD) is a key parameter of any broadband optical device. Since it determines the efficiency of many nonlinear optical processes, its analysis and engineering are of key interest, particularly in the context of novel, miniaturized coherent light sources. Such devices exploit optical nonlinearities either to operate at exotic wavelengths, or to equalize the spacing of optical modes that are otherwise dispersed to form an optical frequency comb (OFC).

Considerable attention has been devoted to studying and optimizing the GVD in semiconductor quantum cascade lasers (QCLs) emitting in the mid- and far-infrared spectral regions.[1–5] These unipolar chip-scale devices offer broadband (100 cm^{-1}/3 THz) coherent OFC generation from an electrically-pumped structure[6] with watt-level power and operation to longer wavelengths. Unfortunately, prior research has shown that stable OFC formation in a QCL cavity

[1]Mahmood.bagheri@jpl.nasa.gov

requires low dispersion in the 100's of fs^2/mm range. This is because a high GVD disperses the modal spacing (so they are not equidistant), causing a loss of OFC properties. While even a more dispersive cavity can sometimes operate as a comb under specific temperature and bias conditions, it becomes weak and difficult to control. The result has been a surge of activity to "dispersion engineer" THz[1,7] and mid-infrared QCLs,[2–5] with the objective of providing broadband, stable OFC emission over a wide range of temperatures and currents.

An alternative semiconductor mid-IR laser OFC platform has recently emerged, based on interband cascade lasers (ICLs).[8–10] This source merges the concepts of cascading from the QCL with interband (electron-hole) transitions from diode lasers, to provide power-efficient generation of midwave-infrared light with low threshold in the 3–6 µm region.[11,12] Intracavity nonlinearities enable self-starting OFC generation with optical bandwidths reaching ~1 THz, which is perfectly suitable for free-running multi-heterodyne experiments. Although ICL combs have already been used in a number of proof-of-concept experiments,[9,13,14] including self-contained room-temperature dual-comb spectroscopy,[15] at this point their spectral properties fall short of other smooth-spectral-envelope chip-scale OFC devices.[16] Here we analyze the origin of these imperfections, by studying different ICL designs with varying ridge widths. Potential strategies for improving the spectral properties will also be presented.

Comb operation at shorter mid-IR wavelengths is especially challenging from a dispersion management standpoint. ICL combs employ the GaSb material system, whose dispersion in the 3–4 µm region is highly positive and ranges between hundreds to more than a thousand fs^2/mm on the short-wavelength side. Furthermore, the narrow ridges required for operation in a single spatial mode induce an additional highly positive dispersion, which increases the typical net GVD value to the 1500–2500 fs^2/mm range. This starkly contrasts the InP platform of QCLs, which contributes negative dispersion above 5 µm. Since this easily compensates the positive waveguide dispersion, it is much more straightforward to engineer a near-zero GVD value that facilitates OFC formation. This is why the majority of mid-IR QCL combs have been developed for the λ = 7–9 µm range.[6,17,18]. Attempts to reach shorter wavelengths have required more complex waveguide engineering[1,3,4] or the deposition of chirped (Gires-Turnois interferometer, GTI) mirrors,[2,19,20] which complicates the device fabrication and may potentially introduce reliability issues. However, the ICL platform provides another interesting mechanism that affects the gain and dispersion in a resonant way, and is therefore potentially useful for local dispersion compensation.

2. MODAL LEAKAGE

Because the ICL's GaSb substrate has a higher refractive index than the modal index, the optical field may penetrate a thin cladding layer and "leak" into the transparent substrate. While the loss of mode confinement has relatively little impact on the lasing threshold,[21] the parasitic vertical cavity formed between the thick (100–150 µm) substrate and the metal bottom contact introduces spectral interference effects. In some devices it leads to severe spectral modulation and mode grouping, with spacing defined by the substrate thickness. Reflection from the top contact may introduce a similar phenomenon,[22] with both yielding quasi-periodic gain and dispersion spectra. These effects were observed in the early days of ICLs[23–25] and many other types of semiconductor lasers,[22,26–28] yet their influence on the dispersion properties has not been studied to date. Surprisingly, intentional modal leakage can be seen as a vertical GTI mirror (short resonant cavity). When carefully designed, it can potentially compensate even for extreme material and waveguide dispersions.

To study the gain and dispersion of unoptimized ICL combs, we biased devices below threshold (~0.95 I_{th}) and measured the amplified spontaneous emission spectrum (ASE) using a Fourier Transform infrared spectrometer (FTIR).[29] The acquired interferograms contain a symmetric center burst around the zero path difference (ZPD) point, along with a satellite burst carrying information about the amplitude and phase spectrum after one round trip. We retrieved the laser gain from the ratio of amplitude spectra for the two bursts. The second derivative of the round trip phase spectrum is the group delay dispersion (GDD), which when normalized to twice the cavity length becomes the GVD. The Fourier transform of a full-length signal (containing both bursts) yields a mode-resolved ASE spectrum.[29]

Figure 1 plots results for two ICLs with similar emission wavelengths (3.33 µm and 3.22 µm) and structural designs following Ref. [30]. Both devices had ridge widths of 3 µm to ensure operation in a single spatial mode. Although the first device (a,c) shows a relatively smooth ASE spectrum, some oscillations with ~15 cm^{-1} period are already visible

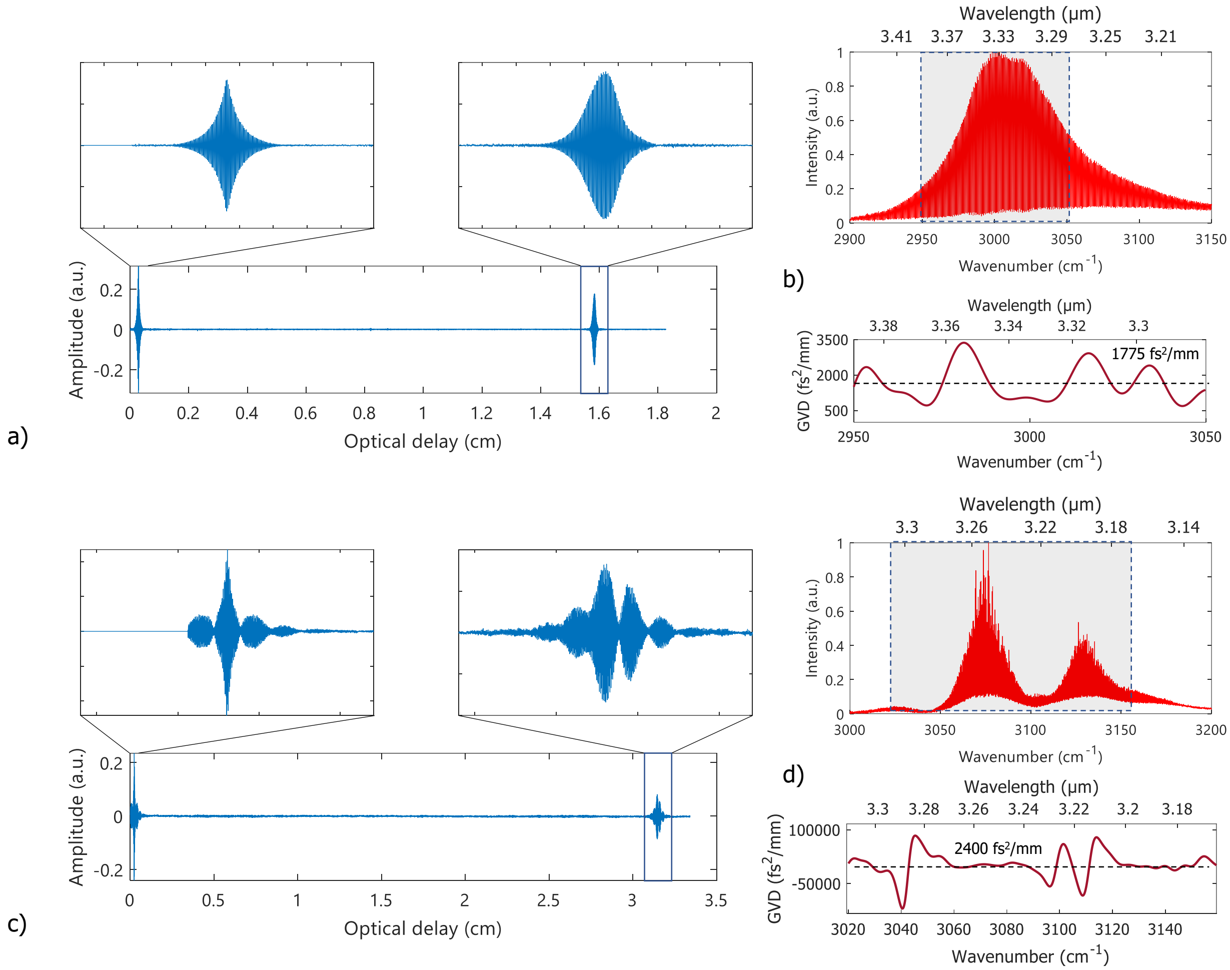

Figure 1. (a,c) Measured sub-threshold interferograms (IFG) for two ICLs; (b,d) corresponding amplified spontaneous emission (ASE) and GVD spectra: The ASE spectrum in (a) is smooth without significant leaky-mode anomalies, whereas in (c) it is extremely modulated. Zoomed panels of the interferograms show symmetric center bursts (left) along with asymmetric satellite (roundtrip) bursts (right). The mode-resolved ASE spectra were calculated from the full-length IFGs. Framed parts of the ASE spectrum were used for the GVD calculations.

in the GVD profile. Whereas a 20 cm^{-1} wide moderate (1000 fs^2/mm) GVD region can be observed around the ASE peak, unfortunately this value rarely yields a low-noise comb spectrum. Instead, the kilohertz to sub-megahertz linewidths for the microwave intermode beat notes are far larger than the sub-kHz values for the best devices.[8,13] The round trip burst of the first device already shows weak asymmetry, and reveals that lower frequencies travel at higher speeds corresponding to a positive dispersion. In contrast, the second device shows an extremely modulated ASE spectrum with a dominant 60 cm^{-1} period. The roundtrip interferogram burst has an extremely asymmetric shape with pulse separation matching the modal group spacing. Obviously, this device displays strong oscillations in both gain and dispersion.

It is important to note here that the processing of these two devices was nearly the same. However, we learned empirically that even a slight changes in the substrate surface quality, after it was to a 100–150 µm thickness, can make two similarly-processed devices perform quite differently. Therefore, a technique for suppressing leakage into the substrate (apart from growing a thicker clad bottom cladding layer[31]) is to make the bottom contact more diffuse by lapping the substrate with a coarser-grit polish prior to deposition of the contact. While the devices studied here were polished using an Al_2O_3 powder with 5 µm particle size, preliminary experiments show effective leakage suppression when the particle size is increased to 14 µm or more. On one hand the lack of leakage helps to flatten the gain and

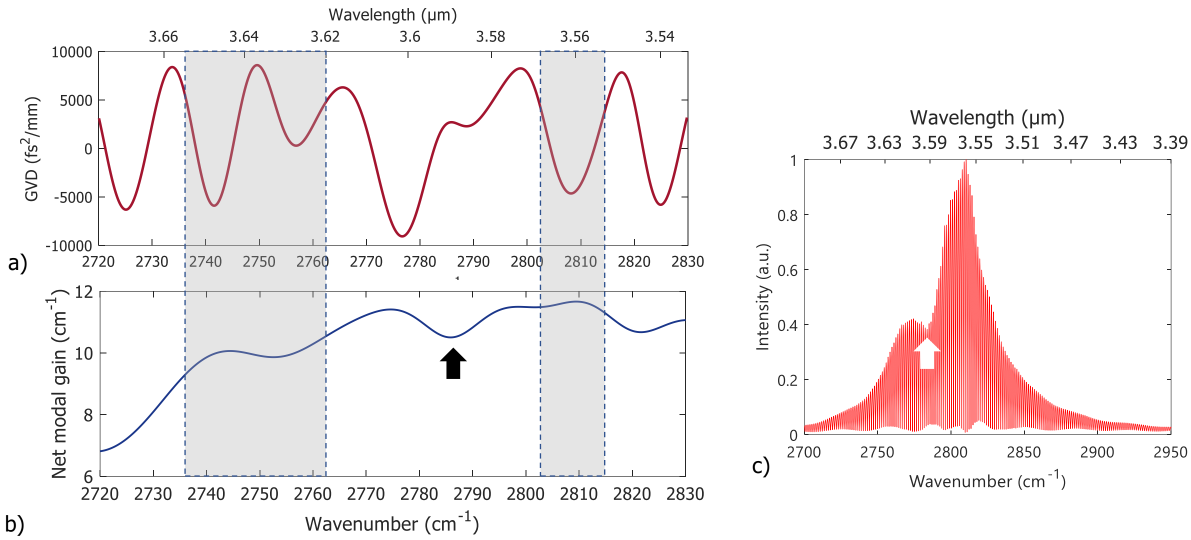

Figure 2. a) Group velocity dispersion (GVD); b) Net modal gain; and c) ASE spectrum of a device with spectral bi-modality, measured at $0.95J_{th}$ and 30°C. The arrow in (b) indicates a dip in the gain and sub-threshold spectrum that creates quite significant oscillations in the dispersion. The framed regions correspond to optical frequencies occupied by laser modes. Note that the sub-threshold analysis does not fully explain the dispersion dynamics of the device, *i.e.*, how it evolves *above* threshold.

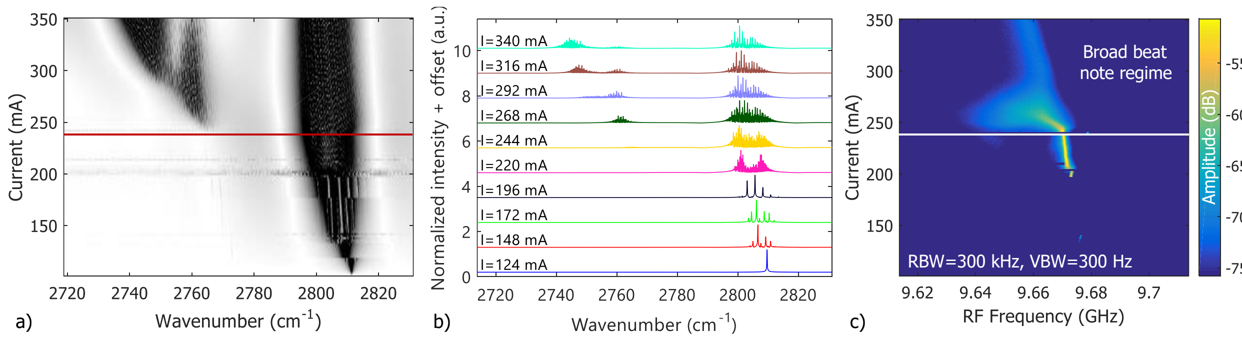

Figure 3. a) Spectral map above threshold for the same device as in Fig. 2. b) Normalized spectra at different injection currents (plotted with an offset). c) Electrical intermode beat note map. Note the significant RF line broadening when a second spectral lobe develops. Due to the large difference in GVDs, the device cannot maintain stable frequency comb generation for both spectral regions simultaneously.

dispersion curves, while on the other the dispersion remains intrinsically high due to material and waveguide dispersion.

3. EFFECT OF LEAKAGE ON COMB OPERATION

To prove that the sub-threshold analysis is meaningful, and to help identify anomalous comb operation regions, we studied how the optical and microwave spectra evolve above threshold. For this we tested a device similar to that presented in Ref. [8], which operated at 3.6 μm with a maximum output power per facet of 10 mW. Note that the comb devices in this study were operated in a frequency modulated (FM) state with the short section of the cavity unbiased. This means that no pulses were generated. Instead, the instantaneous light intensity was almost constant. Figure 2 shows the ASE, gain, and dispersion spectra for this device. Modal leakage is manifested as a moderate dip in the ASE (Fig. 2c, white arrow), which divides the spectrum into partially-overlapping peaks separated by ~30 cm^{-1}. The spacing agrees with previous reports of 20–30 cm^{-1} for substrates 150 ± 20 μm thick. Quasi-periodicity with the same interval

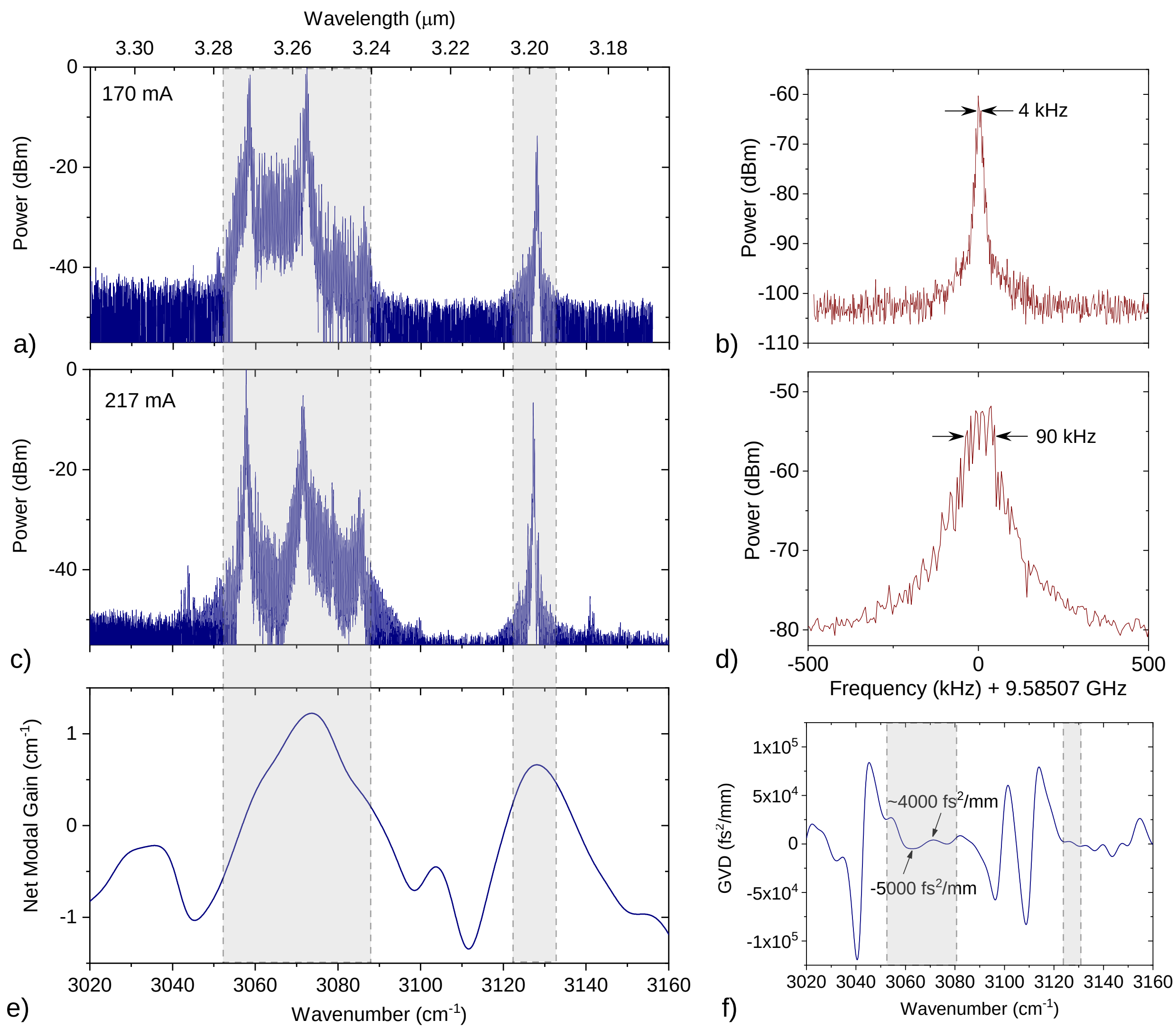

Figure 4. Ultra-broadband (80 nm, or 2.4 THz) ICL comb designed for methane sensing. a) Optical spectrum measured by an OSA in a narrow intermode beat note regime with 10 mW of optical power; b) Corresponding intermode beat note with ~4 kHz 3 dB linewidth; c) Optical spectrum at a slightly higher current; d) Microwave intermode beat note spectrum showing pronounced phase noise; e) Gain profile retrieved from the ASE interferogram; f) Calculated GVD. Note the good agreement between the gain shape and spectral envelope above threshold (shaded regions).

is also observed in the gain spectrum of Fig. 2b. The GVD in Fig. 2a has a shorter (15 cm^{-1}) oscillation period, associated with the second derivative nature of the phase spectrum.

It is interesting that the region identified by the arrow in Fig. 2b is not occupied by lasing modes at all. Instead, the spectrum above threshold (Fig. 3a) splits into two groups (shaded regions in Fig. 2) with dissimilar and rapidly-oscillating group velocity dispersions. Figure 3b shows that at currents below 200 mA, sparse spectra are produced

with relatively few lines and occasional narrow intermode beat notes signifying comb operation. More uniform, denser spectra can also be produced (above 220 mA), albeit with a broader noise pedestal of the microwave intermode beat note (IBN) detected electrically from the ICL. Above 250 mA, when the second spectral group appears, the laser enters a broad IBN regime with multi-megahertz linewidths. It is clear from this example that the sub-threshold analysis helps to identify anomalies in the gain spectrum, which can be used to explain the unusual evolution of the optical and microwave spectra.

Figure 4 illustrates that a similar analysis has been performed on ICLs designed for comb operation around 3.27 μm – the region relevant for methane sensing. As in the case of the previous example, the sub-threshold gain spectrum (Fig. 4e) can explain the anomalous spectral envelope above threshold (Fig. 4a,c). It is surprising that the laser can maintain a narrow IBN linewidth (4 kHz) while emitting light over more than 80 nm (2.4 THz). While a further increase in the current (Figs. 4c,d) leads to an even broader total optical spectrum, the phase noise properties are much worse. Whereas such devices are generally perceived as unsuitable for spectroscopy experiments, due to the extreme non-uniformity of the modal intensities, the large separation of the mode groups may become useful for terahertz generation. The recent discovery of near IR comb emission from an ICL by second-harmonic generation[14] may pave the way to a room-temperature THz comb source that relies on intracavity difference frequency generation (DFG), as was demonstrated previously for QCLs[32,33].

4. MULTIMODE OPERATION

Although there is significant evidence supporting the modal leakage theory, the presence of higher-order lateral modes in the cavity might alternatively explain the mode grouping and heavy modulation of the ASE spectrum. Since the modal indices and GVDs of higher-order modes differ significantly from those of the fundamental, their presence can also degrade the comb's phase-locking properties. However, it can be challenging to determine unambiguously whether higher-order modes are present, because technical artifacts in the FTIR measurement can introduce non-physical lines due to signal path nonlinearities, or they can distort the spectral shape due to incorrect Fourier transformation or aliasing. For this reason, we employed a grating-type mid-IR optical spectrum analyzer with 0.1 nm resolution to confirm the validity of prior analyses based on FTIR data, by determining whether any lasing occurred in higher-order lateral modes. The single-section Fabry-Pérot ICLs with ridge widths varying from 3 to 6.3 μm had cavity lengths of 1 mm, which provided mode spacings of 1.4 nm (1.29 cm^{-1}). The devices mounted on BeO submounts were biased with currents up to ~$9I_{th}$, and operated at temperatures from 10 to 30°C.

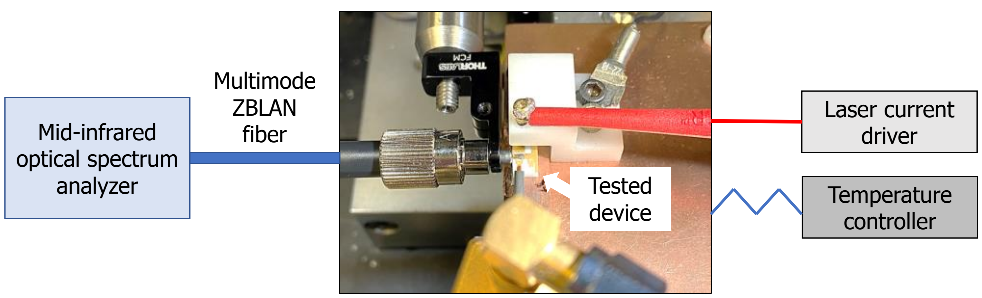

Figure 5. Experimental setup of a mid-infrared optical spectrum analyzer for detecting the presence of higher-order lateral modes in an ICL comb.

Figure 5 shows the experimental setup. Light from the device under test was butt-coupled to a multimode fluoride glass (ZrF_4) fiber, whose large core diameter (100 μm) facilitated efficient collection from the narrow ICL ridge. The fiber ferrule was separated from the facet by approximately 100 μm, and axially positioned to minimize the optical feedback. For that configuration, the emission spectrum at the highest injection current did not change as the fiber was moved away from the facet (at the expense of lower coupling efficiency). With the optical spectrum analyzer operating in slow-scan mode to ensure a high signal-to-noise ratio, it took approximately one minute to record a single spectrum.

Figure 6 shows that only the broadest (6.3 μm) of the ICL ridges lased in multiple lateral modes, which appear only at the highest injection currents (>$8I_{th}$). We see that the optical frequencies of the higher-order modes are detuned significantly from the fundamental, simply because their free spectral range (FSR) is different so they lase at different frequencies. This is especially visible in Fig. 6d.

The multi-mode behavior can be attributed to lateral spatial hole burning (SHB). At sufficiently high optical power, strong stimulated emission into the fundamental mode depletes the carrier population in the center of the ridge enough to permit additional lasing in higher-order modes. This occurs more easily in a broader ridge, and at higher injection

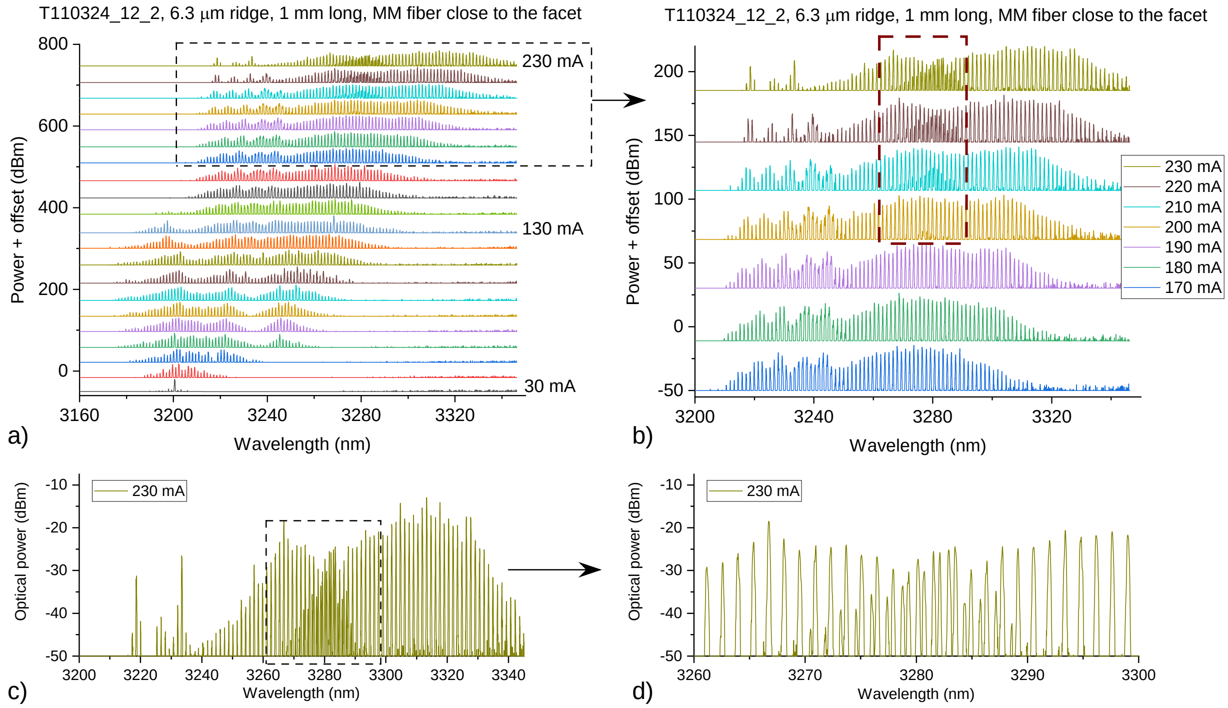

Figure 6. Spectral characteristics of the broadest (6.3 µm wide) ICL ridge, which emitted in multiple lateral modes, albeit only at the highest injection currents (~8×J_{th}). a) Evolution of the optical spectrum. b) Zoom on the highest-current region, where multi-mode behavior becomes visible. c) Spectrum at 230 mA (~9×J_{th}), where an additional set of lines developed around 3280 nm (3049 cm^{-1}). None of the devices with narrower ridges showed such characteristics.

currents. Since the ICL frequency combs reported to date have typically used ridge widths of 3–3.5 µm, which were biased at no more than 5 times the threshold, it appears that lateral multi-mode lasing can be ruled out as a plausible explanation for the spectral anomalies observed above threshold. Nevertheless, this analysis suggests that wider ridges with lower waveguide-induced GVDs may be useful in the future as a tool for dispersion compensation.

5. CONCLUSION

We experimentally investigated the waveguiding and group velocity dispersion properties of interband cascade laser frequency combs. The analysis indicates that modal leakage into the high-index GaSb substrate is responsible for the quasi-periodic modulation observed in the gain and dispersion spectra, with period defined by the substrate thickness. The average group velocity dispersion (GVD) ranges from 1500 to 2500 fs^2/mm, although leakage-induced fluctuations can cause it to drop close to zero in some regions. We also find that narrowing the ridge to <6 µm prevents higher-order lateral modes from appearing in the optical spectra. Future research will focus on investigations of the far-field beam profile to confirm whether broader ridges can be used for ICL combs. Whereas the sub-threshold dispersion analysis has clarified some anomalies in the optical and radio frequency properties, time-domain studies using pump-probe spectroscopic techniques may be needed to fully understand the dispersion dynamics above threshold.[34]

Acknowledgements This work was supported under and was in part performed at the Jet Propulsion Laboratory (JPL), California Institute of Technology, under contract with NASA (PICASSO program 106822/811073.02.24.01.85). L. A. Sterczewski's research was supported by an appointment to the NASA Postdoctoral Program at JPL, administered by Universities Space Research Association under contract with NASA. The NRL authors acknowledge support from the Office of Naval Research (ONR).

REFERENCES

[1] Burghoff, D., Kao, T.-Y., Han, N., Chan, C. W. I., Cai, X., Yang, Y., Hayton, D. J., Gao, J.-R., Reno, J. L. and Hu, Q., "Terahertz laser frequency combs," Nat Photon **8**(6), 462–467 (2014).

[2] Villares, G., Riedi, S., Wolf, J., Kazakov, D., Süess, M. J., Jouy, P., Beck, M. and Faist, J., "Dispersion engineering of quantum cascade laser frequency combs," Optica **3**(3), 252 (2016).

[3] Bidaux, Y., Sergachev, I., Wuester, W., Maulini, R., Gresch, T., Bismuto, A., Blaser, S., Muller, A. and Faist, J., "Plasmon-enhanced waveguide for dispersion compensation in mid-infrared quantum cascade laser frequency combs," Optics Letters **42**(8), 1604 (2017).

[4] Bidaux, Y., Kapsalidis, F., Jouy, P., Beck, M. and Faist, J., "Coupled-Waveguides for Dispersion Compensation in Semiconductor Lasers," Laser & Photonics Reviews **12**(5), 1700323 (2018).

[5] Lu, Q. Y., Manna, S., Slivken, S., Wu, D. H. and Razeghi, M., "Dispersion compensated mid-infrared quantum cascade laser frequency comb with high power output," AIP Advances **7**(4), 045313 (2017).

[6] Hugi, A., Villares, G., Blaser, S., Liu, H. C. and Faist, J., "Mid-infrared frequency comb based on a quantum cascade laser," Nature **492**(7428), 229–233 (2012).

[7] Rösch, M., Beck, M., Süess, M. J., Bachmann, D., Unterrainer, K., Faist, J. and Scalari, G., "Heterogeneous terahertz quantum cascade lasers exceeding 1.9 THz spectral bandwidth and featuring dual comb operation," Nanophotonics **7**(1), 237–242 (2018).

[8] Bagheri, M., Frez, C., Sterczewski, L. A., Gruidin, I., Fradet, M., Vurgaftman, I., Canedy, C. L., Bewley, W. W., Merritt, C. D., Kim, C. S., Kim, M. and Meyer, J. R., "Passively mode-locked interband cascade optical frequency combs," Scientific Reports **8**(1), 3322 (2018).

[9] Sterczewski, L. A., Westberg, J., Patrick, L., Soo Kim, C., Kim, M., Canedy, C. L., Bewley, W. W., Merritt, C. D., Vurgaftman, I., Meyer, J. R. and Wysocki, G., "Multiheterodyne spectroscopy using interband cascade lasers," Optical Engineering **75**(1), 011014 (2017).

[10] Schwarz, B., Hillbrand, J., Beiser, M., Andrews, A. M., Strasser, G., Detz, H., Schade, A., Weih, R. and Höfling, S., "Monolithic frequency comb platform based on interband cascade lasers and detectors," Optica **6**(7), 890–895 (2019).

[11] Yang, R. Q., "Infrared laser based on intersubband transitions in quantum wells," Superlattices and Microstructures **17**(1), 77–83 (1995).

[12] Meyer, J., Vurgaftman, I., Yang, R. and Ram-Mohan, L., "Type-II and type-I interband cascade lasers," Electronics Letters **32**(1), 45–46 (1996).

[13] Sterczewski, L. A., Westberg, J., Bagheri, M., Frez, C., Vurgaftman, I., Canedy, C. L., Bewley, W. W., Merritt, C. D., Kim, C. S., Kim, M., Meyer, J. R. and Wysocki, G., "Mid-infrared dual-comb spectroscopy with interband cascade lasers," Optics Letters **44**(8), 2113–2116 (2019).

[14] Sterczewski, L. A., Bagheri, M., Frez, C., Canedy, C. L., Vurgaftman, I., Kim, M., Kim, C. S., Merritt, C. D., Bewley, W. W. and Meyer, J. R., "Near-infrared frequency comb generation in mid-infrared interband cascade lasers," Opt. Lett. **44**(23), 5828–5831 (2019).

[15] Sterczewski, L. A., Bagheri, M., Frez, C., Canedy, C. L., Vurgaftman, I. and Meyer, J. R., "Mid-infrared dual-comb spectroscopy with room-temperature bi-functional interband cascade lasers and detectors," Appl. Phys. Lett. **116**(14), 141102 (2020).

[16] Scalari, G., Faist, J. and Picqué, N., "On-chip mid-infrared and THz frequency combs for spectroscopy," Applied Physics Letters **114**(15), 150401 (2019).

[17] Lu, Q., Wu, D., Slivken, S. and Razeghi, M., "High efficiency quantum cascade laser frequency comb," Scientific Reports **7**, 43806 (2017).

[18] Jouy, P., Wolf, J. M., Bidaux, Y., Allmendinger, P., Mangold, M., Beck, M. and Faist, J., "Dual comb operation of $\lambda \sim 8.2$ μm quantum cascade laser frequency comb with 1 W optical power," Applied Physics Letters **111**(14), 141102 (2017).

[19] Gires, F. and Tournois, P., "Interferometre utilisable pour la compression dimpulsions lumineuses modulees en frequence," Comptes Rendus Hebdomadaires Des Seances De L Academie Des Sciences **258**(25), 6112 (1964).

[20] Lu, Q. Y., Manna, S., Wu, D. H., Slivken, S. and Razeghi, M., "Shortwave quantum cascade laser frequency comb for multi-heterodyne spectroscopy," Applied Physics Letters **112**(14), 141104 (2018).

[21] Vurgaftman, I., Weih, R., Kamp, M., Meyer, J. R., Canedy, C. L., Kim, C. S., Kim, M., Bewley, W. W., Merritt, C. D., Abell, J., and S Höfling., "Interband cascade lasers," J. Phys. D: Appl. Phys. **48**(12), 123001 (2015).

[22] Arzhanov, E. V., Bogatov, A. P., Konyaev, V. P., Nikitina, O. M. and Shveikin, V. I., "Waveguiding properties of heterolasers based on InGaAs/GaAs strained quantum-well structures and characteristics of their gain spectra," Quantum Electron. **24**(7), 581–587 (1994).
[23] Suchalkin, S., Bruno, J., Tober, R., Westerfeld, D., Kisin, M. and Belenky, G., "Experimental study of the optical gain and loss in InAs/GaInSb interband cascade lasers," Appl. Phys. Lett. **83**(8), 1500–1502 (2003).
[24] Canedy, C. L., Boishin, G. I., Bewley, W. W., Kim, C. S., Vurgaftman, I., Kim, M., Lindle, J. R., Meyer, J. R. and Whitman, L. J., "Correlating growth conditions with photoluminescence and lasing properties of mid-IR antimonide type II 'W' structures," J. Vac. Sci. Technol. B **22**(3), 1575 (2004).
[25] Bewley, W. W., Canedy, C. L., Kim, C. S., Vurgaftman, I., Kim, M. and Meyer, J. R., "Antimonide type-II 'W' lasers: growth studies and guided-mode leakage into substrate," Physica E: Low-dimensional Systems and Nanostructures **20**(3–4), 466–470 (2004).
[26] O'Reilly, E. P., Onischenko, A. I., Avrutin, E. A., Bhattacharyya, D. and Marsh, J. H., "Longitudinal mode grouping in InGaAs/GaAs/AlGaAs quantum dot lasers: Origin and means of control," Electron. Lett. **34**(21), 2035 (1998).
[27] Smowton, P. M., Johnston, E. J., Dewar, S. V., Hulyer, P. J., Summers, H. D., Patanè, A., Polimeni, A. and Henini, M., "Spectral analysis of InGaAs/GaAs quantum-dot lasers," Appl. Phys. Lett. **75**(15), 2169–2171 (1999).
[28] Bhattacharyya, D., Avrutin, E. A., Bryce, A. C., Marsh, J. H., Bimberg, D., Heinrichsdorff, F., Ustinov, V. M., Zaitsev, S. V., Ledentsov, N. N., Kop'ev, P. S., Alferov, Zh. I., Onischenko, A. I. and O'Reilly, E. P., "Spectral and dynamic properties of InAs-GaAs self-organized quantum-dot lasers," IEEE J. Select. Topics Quantum Electron. **5**(3), 648–657 (1999).
[29] Hofstetter, D. and Faist, J., "Measurement of semiconductor laser gain and dispersion curves utilizing Fourier transforms of the emission spectra," IEEE Photonics Technology Letters **11**(11), 1372–1374 (1999).
[30] Canedy, C. L., Abell, J., Merritt, C. D., Bewley, W. W., Kim, C. S., Kim, M., Vurgaftman, I. and Meyer, J. R., "Pulsed and CW performance of 7-stage interband cascade lasers," Optics Express **22**(7), 7702 (2014).
[31] Vurgaftman, I., Bewley, W. W., Canedy, C. L., Kim, C. S., Kim, M., Ryan Lindle, J., Merritt, C. D., Abell, J. and Meyer, J. R., "Mid-IR Type-II Interband Cascade Lasers," IEEE J. Select. Topics Quantum Electron. **17**(5), 1435–1444 (2011).
[32] Belkin, M. A., Capasso, F., Xie, F., Belyanin, A., Fischer, M., Wittmann, A. and Faist, J., "Room temperature terahertz quantum cascade laser source based on intracavity difference-frequency generation," Appl. Phys. Lett. **92**(20), 201101 (2008).
[33] Lu, Q., Wang, F., Wu, D., Slivken, S. and Razeghi, M., "Room temperature terahertz semiconductor frequency comb," 1, Nature Communications **10**(1), 2403 (2019).
[34] Burghoff, D., Yang, Y., Reno, J. L. and Hu, Q., "Dispersion dynamics of quantum cascade lasers," Optica **3**(12), 1362 (2016).